

DIRECT INK WRITING OF FLEXIBLE PIEZOELECTRIC SENSORS

by

Amanda M White



A thesis

submitted in partial fulfillment

of the requirements for the degree of

Master of Science in Mechanical Engineering

Boise State University

December 2022

© 2022

Amanda M White

ALL RIGHTS RESERVED

BOISE STATE UNIVERSITY GRADUATE COLLEGE

DEFENSE COMMITTEE AND FINAL READING APPROVALS

of the thesis submitted by

Amanda M White

Thesis Title: Direct Ink Writing of Flexible Piezoelectric Sensors

Date of Final Oral Examination: 18 October 2022

The following individuals read and discussed the thesis submitted by student Amanda M White, and they evaluated the student's presentation and response to questions during the final oral examination. They found that the student passed the final oral examination.

Zhangxian Deng, Ph.D. Chair, Supervisory Committee

Dave Estrada, Ph.D. Member, Supervisory Committee

Gunes Uzer, Ph.D. Member, Supervisory Committee

The final reading approval of the thesis was granted by Zhangxian Deng, Ph.D., Chair of the Supervisory Committee. The thesis was approved by the Graduate College.

DEDICATION

I dedicate my thesis work to my family and friends who have been a constant source of support and encouragement during the challenges of graduate school and life. I would also like to dedicate this thesis to my fellow graduate student and friend David Vogel who would have graduated with me. May your memory be forever held within these pages.

ACKNOWLEDGMENTS

I would like to express my deepest appreciation to my adviser Dr. Zhangxian Deng. His constant support and encouragement motivated me to push past any challenge and to have confidence in myself always.

I would also like to acknowledge my committee members, Dr. Gunes Uzer and Dr. David Estrada. Thank you for your commitment and support.

Lastly, I would like to acknowledge my research team for assisting me along the way. Thank you to Nick McKibben, Shane Palmer, Braden Robinson, Terek Zimmerman, Adam Tran, Fereshteh Rajabi Kouchi, Joy Morin, Drew Keller, Vaughn Pollock, Joshua Poorbaugh and Anastasiya Artyukhov.

ABSTRACT

Piezoelectric poly(vinylidene fluoride-co-trifluoroethylene), or PVDF-trFE, builds up significant electrical charges on its surface when stressed. By correlating the mechanical force with the resulting electrical charges or voltages, researchers have developed flexible, broadband, and biocompatible force sensors. PVDF-trFE force sensors are traditionally fabricated via spin coating or solvent casting, which result in large waste production and experience difficulties in forming complex geometries. To tackle these challenges, I leveraged a commercial direct ink writing system (nScript microdispenser) to additively manufacture PVDF-trFE force sensors. I first synthesized an unprecedented piezoelectric ink that is compatible with a commercial ink writing system at Boise State University, specifically the nScript microdispenser, by dissolving PVDF-trFE powders into a cosolvent system consisting of methyl ethyl ketone and dimethyl sulfoxide. The ink composition and substrate surface properties were optimized simultaneously to ensure consistent and uniform printing. Postprocessing procedures, including air-drying, thermal curing, electrical poling and non-contact corona poling were then investigated to facilitate polymerization and beta phase transformation in the printed PVDF-trFE films. With the knowledge acquired from these investigations, I prototyped a piezoelectric force sensor consisting of printed PVDF-trFE films and printed silver electrodes. From justifying the methods for sensor fabrication, unprecedented prototypes of PVDF-trFE sensor arrays were investigated.

TABLE OF CONTENTS

DEDICATION	iv
ACKNOWLEDGMENTS	v
ABSTRACT	vi
LIST OF TABLES	ix
LIST OF FIGURES	x
LIST OF ABBREVIATIONS	xii
CHAPTER ONE: INTRODUCTION	1
Overview	1
Motivation	1
Intellectual Merit	3
Broader Impacts	4
CHAPTER TWO: BACKGROUND	6
Piezoelectric Materials	6
Piezoelectric Sensor Configuration	7
Direct Ink Writing	8
CHAPTER THREE: RESEARCH DESIGN	10
Objective 1: Print Uniform PVDF-trFE Films	10
Summary	10
Completed Work	10

Future Work.....	18
Objective 2: Investigate Effect of Printing Parameters	19
Summary	19
Completed Work.....	19
Future Work.....	23
Objective 3: Optimize Post-Processing Procedures	25
Summary	25
Completed Work.....	25
Future Work.....	31
Objective 4: Prototype and Characterize PVDF-trFE Force Sensors.....	32
Summary	32
Completed Work.....	33
Future Work.....	37
Conclusion	38
REFERENCES	40
APPENDIX	45

LIST OF TABLES

Table 3.1	PVDF-trFE Ink Recipes Developed in this Study.....	11
Table 3.2	Initial Printer Settings for 10 wt.% PVDF-trFE Inks	20
Table 3.3	Optimized Printer Settings for 10 wt.% PVDF-trFE Inks	22
Table 3.4	Optimized Printer Settings for Silver Electrode.....	26
Table A.1	Results of Poling Experiment Conducted at 20 °C and Measured in pC/N	46
Table A.2	Results of Poling Experiment Conducted at 40 °C and Measured in pC/N	47
Table A.3	Results of Poling Experiment Conducted at 60 °C and Measured in pC/N	48

LIST OF FIGURES

Figure 2.1	Dimensions of the PVDF-trFE Force Sensor	8
Figure 2.2	Physical Assembly (Left) and Schematic (Right) of the nScript Microdispenser	9
Figure 3.1	Printed and Annealed PVDF-trFE Films, 10 wt.% (Left) and 20 wt.% (Right)	12
Figure 3.2	Pipette-Casted Droplet Study. Droplets of 10 wt.% PVDF-trFE Ink Mixed in Polystyrene Vial Air-Dried for 0.5-8 Hours.....	12
Figure 3.3	Pipette-Casted Droplet Study. Droplets of 10 wt.% PVDF-trFE Ink Stored in Polystyrene Vial for 0-3 Weeks.....	13
Figure 3.4	Pipette-Casted Droplet Study. Droplets of 10 wt.% PVDF-trFE Ink Mixed in Glass Vial and Air-Dried for 0-24 Hours.....	14
Figure 3.5	Effect of Curing Duration Ranging from 15-60 Minutes.....	15
Figure 3.6	Investigation of Curing Temperature with Optical Images (a, c, e) and Profilometer Measurements (b, d, f). Temperatures Investigated Include 130 °C, 170 °C and 90 °C for (a-b), (c-d) and (e-f) Respectively	17
Figure 3.7	Illustration of Various Contact Angle Measurements.....	18
Figure 3.8	nScript Printed 10 wt.% PVDF-trFE Films Utilizing Initial Printing Parameters from Table 3.2	20
Figure 3.9	Printer Setting Investigation: Average Line Height and Width for Varying (a) Pressure, (b) Speed and (c) Valve Delta	21
Figure 3.10	Map Scan of a 10 mm Diameter PVDF-trFE Print.....	23
Figure 3.11	Illustration of Various Line Spacing for a Printed Design.....	24
Figure 3.12	Comparison of nScript Printed Electrodes for Three Different Silver Inks: (a) Dupont 5029 Ink, (b) Applied Ink Solutions Water-Based Ink, and (c) NovaCentrix Metalon Ink.....	26

Figure 3.13	Electrical Poling in Silicone Oil Bath: (a) Assembly and (b) Schematic ..	28
Figure 3.14	Commercial d33 Measuring Setup	29
Figure 3.15	Results of Electrical Poling Study Analyzing Driving Voltage and Poling Duration Conducted at (a) 20 °C, (b) 40 °C, and (c) 60 °C	30
Figure 3.16	Non-Contact Corona Poling Assembly	32
Figure 3.17	Dimensions of PVDF-trFE 1D 'Piano' Sensor Array	33
Figure 3.18	Custom Characterization Setup of the 1D 'Piano' Sensor Array.....	34
Figure 3.19	Customized Load Frame Setup (a) and Schematic (b) Showing Printed Sensors Sandwiched Between a PZT Actuator and Piezo Force Sensor...35	35
Figure 3.20	Sensitivity (V/N) vs. Frequency (Hz) of nScript Printed, Electrically Poled Sensors Compared to Commercial PVDF-trFE Sensor	36
Figure 3.21	Electrical Response of Printed PVDF-trFE Sensor Over 2 ms at (a) 2 kHz and (b) 5 kHz.....	37
Figure 3.22	2D Sensor Array (a) Schematic and (b) Prototype.....	37

LIST OF ABBREVIATIONS

PVDF-trFE	Polyvinylidene Fluoride-Trifluoroethylene
MEK	Methyl Ethyl Ketone
DMSO	Dimethyl Sulfoxide
TGA	Thermogravimetric Analysis
DSC	Differential Scanning Calorimetry
FTIR	Fourier-Transform Infrared Spectroscopy

CHAPTER ONE: INTRODUCTION

Overview

The goal of this project was to utilize direct ink writing techniques to develop novel flexible piezoelectric sensors. Towards this goal, I accomplished four objectives: (1) print uniform flexible piezoelectric films; (2) understand printer setting effects; (3) optimize piezoelectric film post-processing procedures; (4) characterize resultant piezoelectric sensor prototypes. The final deliverables include a dynamic force sensor that can be directly compared to commercially available products and an unprecedented all-printed piezoelectric tactile sensor array.

Motivation

Mechanical force is usually measured indirectly using capacitive or resistive strain gauges. Capacitive strain gauges consist of a dielectric layer sandwiched by a pair of electrodes. Under mechanical pressure, the thickness of the dielectric layer reduces, and the capacitance measured across the electrodes increases [1]. Resistive strain gauges are made of meandering wires whose dimensions and electrical resistance change due to mechanical forces [2]. Instead of using passive wires that only exhibit resistance variation due to the geometric variation, recent studies used piezoresistive wires to form strain gauges and achieved enhanced sensitivity [3]. These strain gauges have demonstrated feasibility, high temperature tolerance, and mechanical robustness in a wide range of applications. However, capacitive, and resistive strain gauges need to be calibrated regularly due to severe drift and are unsuitable for high frequency measurement. A bridge

circuit along with an external power supply are also required to measure the mechanically induced variations in capacitance and resistance.

PVDF-trFE force sensors were commercially fabricated via solvent casting, spin coating, and screen-printing methods. For simple and small-scale sensor development, these methods have worked well. However, each method limits fabrication efficiency and can be costly. Specifically, solvent casting is not suited for complex structure development. Solvent recovery requires high energy and costly procedures, and drying time is highly dependent on ink volatility [4]. Spin coating is useful for achieving very uniform films; however, complex designs require costly and time-consuming photolithographic techniques as well as produce large amounts of waste [5-6]. Screen printing methods struggle with high batch-to-batch variation, possible contamination, poor precision/quality control and large waste production. Depending on the ink properties, screens also require cleaning between batches and fast-paced work to prevent drying/sticking, making it not ideal for large-scale development [7].

Recent studies have focused on additive manufacturing techniques that can enable rapid prototyping of PVDF-trFE structures in complex geometries while minimizing waste production. Fused filament printing is a fast and simple method in which a wide range of filaments can be utilized. However, this method struggles with print quality, often printing warped samples with holes [8-9]. Electrospinning is another method that is commonly used to produce piezoelectric bioscaffolds, as it makes fiber development simple. However, optimizing the many parameters for this method of printing can become time consuming while still yielding samples with rough surface textures and lower mechanical properties [10-11]. Inkjet printing has become a common method for

depositing PVDF-trFE films. Although this method is simple and requires little oversight, it is extremely limited by ink viscosity, therefore limiting the concentration of PVDF-trFE in inks. This method also works by depositing very thin layers of material, so building up layers to a desired thickness can become very time consuming as well [12-14].

To lift the limitations in film quality, mechanical robustness, and ink viscosity, this project aimed to leverage the direct ink writing technique to additively manufacture piezoelectric PVDF-trFE films along with flexible electrodes. First, I developed an nScript microdispenser compatible PVDF-trFE ink. To optimize the ink for best printability, I tested different weight percentage concentrations of PVDF-trFE powders within the cosolvent system. Then I optimized annealing procedures for printed PVDF-trFE thin films to ensure film uniformity. Afterwards, I completed an investigation of silver inks to determine the best printed electrode material. Once the optimal silver ink was determined, I optimized the electrical poling procedures to best facilitate beta phase transformation. I then characterized the prototyped sensors to confirm that d_{33} values and sensitivity measurements match commercially available products.

Intellectual Merit

From this study, several products may be produced from the acquired knowledge. First, I produced a dynamic piezoelectric force sensor utilizing direct ink writing techniques. Procedures used to create this sensor lift constraints on viscosity, minimize waste production, and produce sensors that can directly measure mechanical stress without constant calibration. Secondly, I produced a tactile sensor array that can not only measure force magnitude but also determine the location of the applied force within the

sensor. These tactile sensors can range in size from a 2x2 orientation and beyond. Third, energy harvesters may be produced utilizing similar processes that were optimized and justified in this study. Fourth, bioscaffolds may be produced utilizing the same direct ink writing techniques that were investigated.

Broader Impacts

In 2018, the PVDF-trFE market reached 746 million USD and is estimated to reach 1.169 billion USD by 2025 [15]. By determining a method for rapid production of PVDF-trFE films, like direct ink writing, the utilization of this material in the development of dynamic force sensors and other products is likely to become especially profitable.

This research also has the potential to impact the research efforts of several other fields. PVDF-trFE is an especially useful material for its biocompatibility and properties. Therefore, optimizing methods for PVDF-trFE printing and beta phase transformation have the potential to aid other researchers in the development of new products without having as many difficulties with film quality, mechanical robustness, ink viscosity and sensitivity. By investigating the potential uses and techniques for nScript microdispensing, fields that otherwise would not pursue direct ink writing methods can be impacted. For instance, bioscaffolds are typically produced by solvent casting and electrospinning methods [16] which have constraints lifted by nScript microdispensing.

Aside from conducting research on direct ink writing of piezoelectric materials, I have had the opportunity to connect with students through my teaching assistantship. Through my assistantship, I have taught students introductory concepts of MATLAB and how to utilize the software to analyze data to answer scientific questions. In teaching

students how to read in and analyze data, I have conveyed many methods that I utilize in my research and how they can be applied to several areas of interest.

CHAPTER TWO: BACKGROUND

Piezoelectric Materials

Piezoelectric materials can directly convert mechanical stimuli into electrical charges without the use of any additional power supplies. The mechano-electrical coupling is also instantaneous. Therefore, previous studies have presented passive and high frequency force sensors based on piezoelectric materials [17-18]. The sensitivity of piezoelectric force sensors is determined by the piezoelectric coefficient, d_{33} , which describes the electrical charges induced by a unit force. Piezoelectric materials have varying d_{33} ranges and mechanical properties. For example, piezoelectric single crystals (e.g., quartz, lithium niobate, alumina nitride) have stable piezoelectric properties, high operating temperatures and high Young's moduli. However, they tend to have low d_{33} values, less than 10 pC/N, and are difficult to deposit into complex designs [19-21]. Conversely, polycrystalline ceramics (e.g., lead zirconate titanate, barium titanate) have d_{33} values, ranging between 200-400 pC/N, respectively, while also having high operating temperatures. However, these ceramic materials have low mechanical strengths and are very brittle, making them not ideal for flexible sensor applications [22-25]. Piezoelectric polymers, including polyvinylidene fluoride (PVDF) and polyvinylidene fluoride-trifluoroethylene (PVDF-trFE) have been found to be ideal for flexible sensor development due to their ductility, high mechanical strength, biocompatibility, and chemical resistance [26-27]. Although both materials are limited by low operating temperatures, PVDF-trFE has shown to have a higher piezoelectricity than its counterpart

with a d_{33} value ranging between 25-30 pC/N [28-29]. Therefore, it has been widely used in healthcare [30-31], and energy scavenge/storage [32-33] areas.

Commercially available PVDF-trFE powders can be purchased in different mol ratios ranging from 80:20 to 55:45. As TrFE mol% increases, an increase in peak dielectric constant can be seen. However, with larger TrFE mol%, peaks are seen at lower operating temperatures and any further increase in temperature yields a lower dielectric constant [34]. Therefore, to develop PVDF-trFE force sensors with the highest operating temperatures, 80:20 mol ratio PVDF-trFE powders were utilized in this study.

Piezoelectric Sensor Configuration

Figure 2.1 shows the dimensions of the PVDF-trFE force sensor I fabricated in this study which consists of a PVDF-trFE film sandwiched between a copper-coated Kapton substrate and a printed silver electrode. The PVDF-trFE layer converts mechanical energy to electrical energy. The resulting electrical voltage measured across the electrodes is proportional to the applied force magnitude [35]. Sheets of 6×6×0.003-inch single sided copper-coated Kapton (Adafruit, product no. 1894) were cut into 1×1 squares and used as sensor substrates due to its high flexibility. The copper coated layer is 35 μm thick.

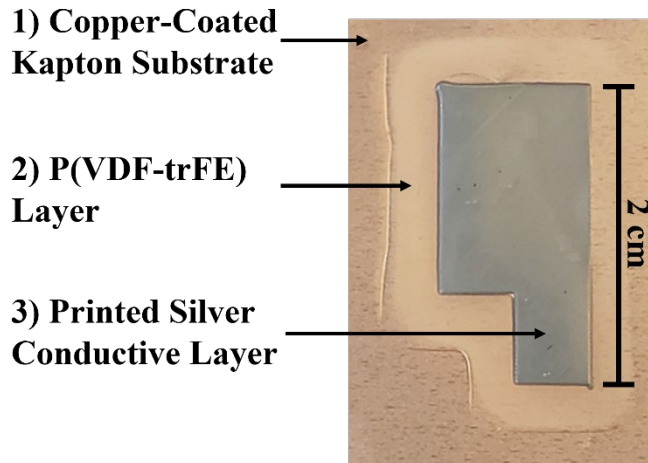


Figure 2.1 Dimensions of the PVDF-trFE Force Sensor

Direct Ink Writing

The nScript Microdispenser (nScript, 150-3Dn-HP), shown in Figure 2.2, is a type of printer that utilizes compressed air to move viscous ink from a syringe through the print head to be deposited in a specific design on any substrate. A valve plunger is utilized to control the ink flow rate. The print head moves vertically to adjust for the gap between the nozzle and the substrate. The substrate is fixed to a motorized micro-stage and moves in a horizontal direction. The quality of printed lines, specifically uniformity and thickness, is controlled by adjusting valve opening, micro-stage speed, and compressed air pressure. Compared to other additive manufacturing techniques, direct ink writing is more economic and efficient in producing large scale PVDF-trFE films with varying thicknesses while lifting the strict constraints on ink viscosity and reducing waste production. This printing method is particularly useful for PVDF-trFE sensor development because it can handle a wide range of viscosities (1-1,000,000 cps) so that both the piezoelectric and electrode layers, consisting of different materials, can be printed using the same setup with little turn-around time and at no cost to the mechanical properties of the printed materials. Complex designs, either 2D or 3D, can be imported

into the nScript software in .dxf format and can be printed relatively quickly depending on the design.

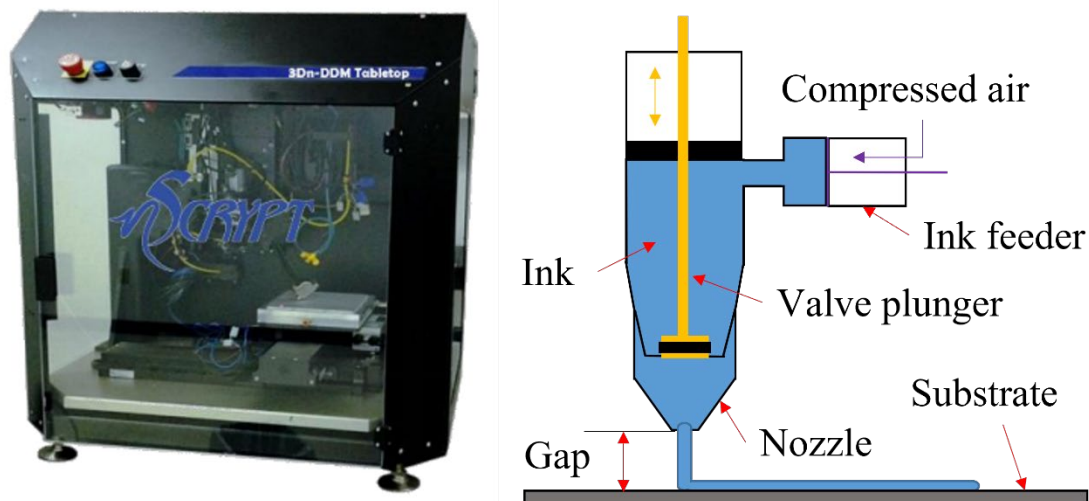


Figure 2.2 Physical Assembly (Left) and Schematic (Right) of the nScript Microdispenser

CHAPTER THREE: RESEARCH DESIGN

Objective 1: Print Uniform PVDF-trFE Films

Summary

To develop uniform printed piezoelectric films, several pre- and post-printing factors were investigated. Towards this objective, several smaller tasks were developed to analyze each factor. Task 1.1 aimed to develop the optimal printable ink recipe for this study. For this task, two recipes of PVDF-trFE ink were developed with varying concentrations of PVDF-trFE powders. These inks were printed via nScript microdispensing and compared. Ink consistency was then measured over time. Task 1.2 aimed to measure the effect of cosolvent evaporation speed from printed films on film uniformity. For this task, an air-drying study was completed. Task 1.3 aimed to investigate the effect of curing duration and temperature. A stylus profilometer was then utilized to measure printed film surface uniformity. The successful completion of this objective was achieved by producing printed PVDF-trFE films, with thickness measurements greater than 20 μm , atop copper-coated Kapton substrates.

Completed Work

Following a successful PVDF-trFE ink recipe developed for inkjet printing [12,36], I developed a viscous PVDF-trFE ink for the nScript microdispenser. PVDF-trFE powders with a PVDF-trFE mole ratio of 80:20 (PolyK Technologies) were dissolved in a cosolvent system consisting of methyl ethyl ketone (MEK) and dimethyl sulfoxide (DMSO), where MEK acts as the main solvent for PVDF-trFE and DMSO

stabilizes the MEK at room temperature. The maximum PVDF-trFE concentration in inkjet inks was 0.8 wt.% due to the strict constraints on ink viscosity. The nScript microdispenser can print inks with a wide range of viscosities (1-1,000,000 cps). Therefore, I developed two inks that contain 10 and 20 wt.% PVDF-trFE, respectively, as shown in Table 3.1.

Table 3.1 PVDF-trFE Ink Recipes Developed in this Study

	Chemical	Weight (g)
10 wt.% Ink	MEK	5.498
	DMSO	15.026
	PVDF-trFE	2.281
20 wt.% Ink	MEK	8.667
	DMSO	11.843
	PVDF-trFE	5.127

All the ink ingredients were mixed in a polystyrene vial using a vortex mixer (Fisherbrand) at a speed level of 4 for approximately 1 hour. To validate their printability, all inks were printed using the nScript microdispenser and then immediately cured in an oven (Heratherm) at 130 °C for 1 hour, per vendor recommendation. As shown in Figure 3.1, the annealed 10 wt.% ink is uniformly distributed throughout the design while the 20 wt.% ink displays air bubbles and dragging along the edges. Due to the visual uniformity difference between the two films, as well as the difficulty experienced while printing the much thicker 20 wt.% ink, I chose to work with the 10 wt.% ink for future development of sensors.

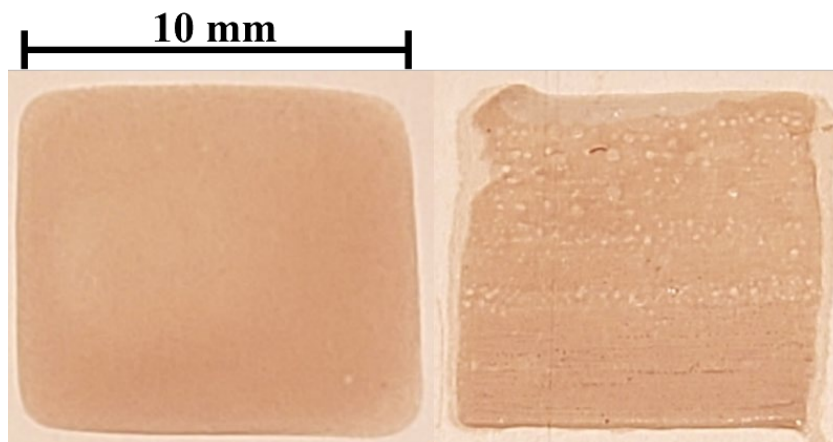


Figure 3.1 Printed and Annealed PVDF-trFE Films, 10 wt.% (Left) and 20 wt.% (Right)

I then conducted an air-drying study in which nScript printing was mimicked by pipette-casting. I pipette-casted 15 μL droplets of the 10 wt.% PVDF-trFE ink on copper-coated Kapton substrates and air dried each droplet for 0.5-8 hours, respectively, under a fume hood. After air-drying, the droplets were then placed in a room temperature oven that was then ramped up to 130 $^{\circ}\text{C}$ and cured for 1 hour. The resulting droplets can be seen in Figure 3.2 in which non-uniformities can be seen in samples dried for less than 5 hours and air-drying for 5 hours and above yielded uniform droplets.

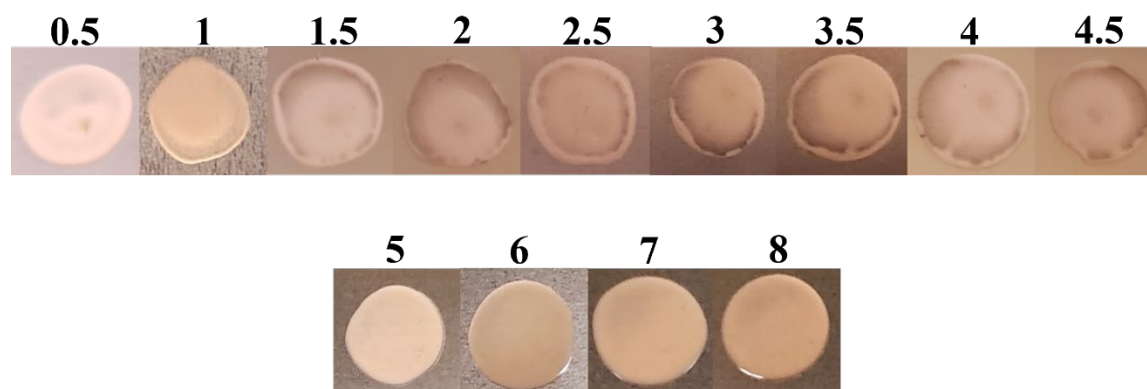


Figure 3.2 Pipette-Casted Droplet Study. Droplets of 10 wt.% PVDF-trFE Ink Mixed in Polystyrene Vial Air-Dried for 0.5-8 Hours

I was able to consistently produce uniform droplets by utilizing a 5 hour air-dry with 1 hour curing at 130 °C. However, after a week, I noticed a change in uniformity despite utilizing the same air-drying and curing conditions. I then performed a consistency study in which I developed a new batch of ink, deposited, air-dried and cured droplets with the same conditions over the span of three weeks in one-week increments. Figure 3.3 shows that, over time, the uniformity of droplets changes significantly. I determined that the Vortex corresponding polystyrene vials, used to mix and store the ink, are not compatible with the chemicals in the cosolvent system. Therefore, over the course of this experiment, polystyrene slowly dissolved into the ink changing its chemical composition. To correct this problem, polystyrene vials were replaced with glass vials which are compatible with the ink solvents.

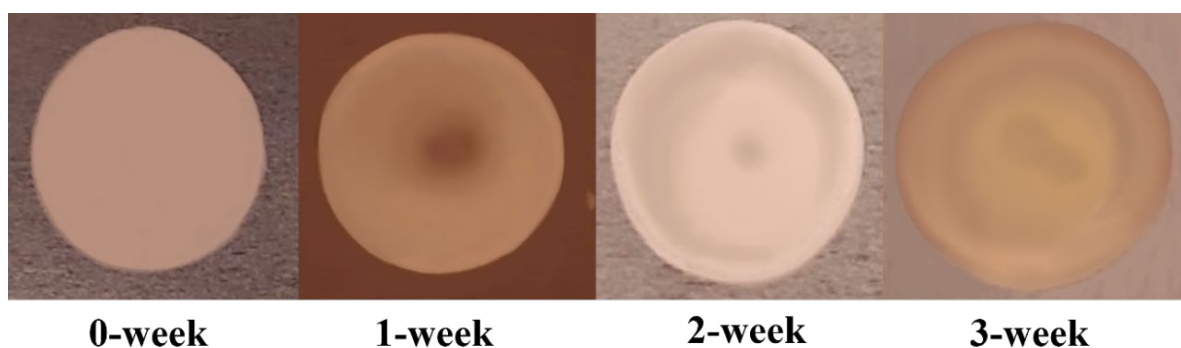


Figure 3.3 Pipette-Casted Droplet Study. Droplets of 10 wt.% PVDF-trFE Ink Stored in Polystyrene Vial for 0-3 Weeks

Utilizing glass vials to mix and store inks, maintaining uncontaminated ink formulation, I reconducted the air-drying study. In this study, I air-dried droplets of PVDF-trFE ink and air-dried for 0-24 hours in 4-hour increments under a fume hood before placing samples in a room temperature oven that would then be ramped up to 130 °C for 1 hour. Additionally, I immediately cured droplets after deposition in an oven that

was pre-heated 130 °C. Figure 3.4 shows the uniformity of these droplets. From this experiment we can see that a 24 hour air-dry completely dries out droplets and causes delamination from the substrate. As droplets were air-dried for less time uniformity increased. Utilizing the pre-heated oven condition, films with the greatest uniformity were developed. This experiment revealed that evaporating the solvents in the ink at a faster rate, by placing droplets in a heated oven, yields more uniform thin films.

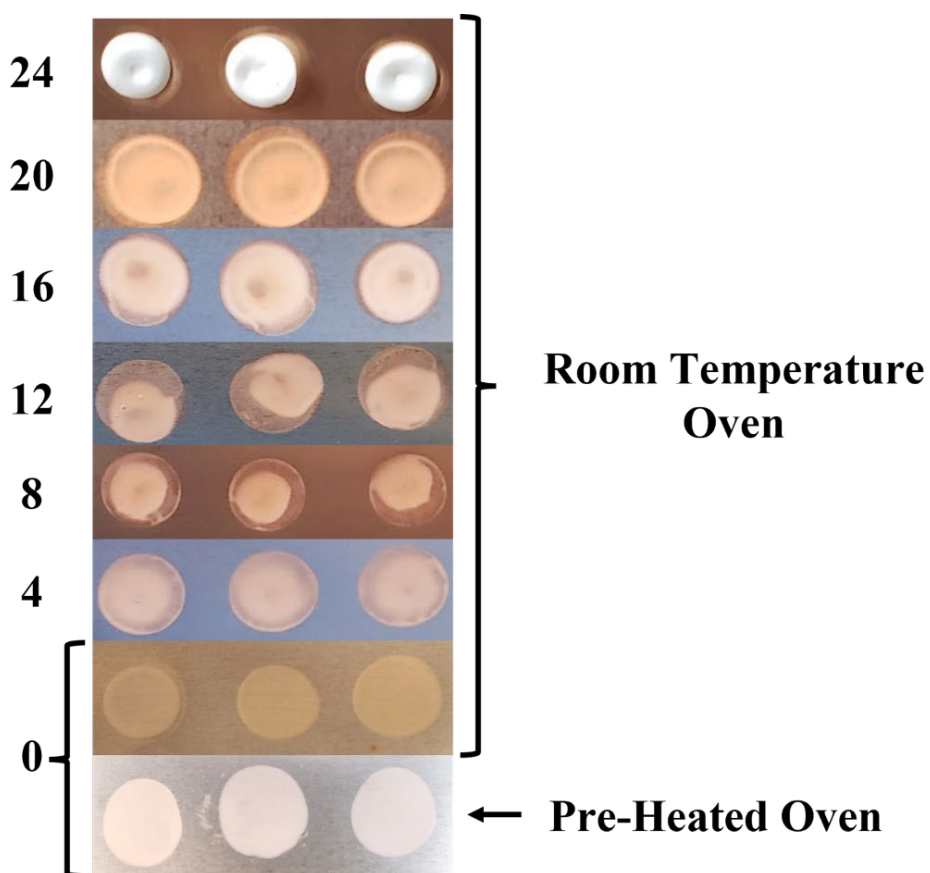


Figure 3.4 Pipette-Casted Droplet Study. Droplets of 10 wt.% PVDF-trFE Ink Mixed in Glass Vial and Air-Dried for 0-24 Hours

I then investigated the effect of each curing parameter on film uniformity. First, I investigated the effect of curing duration. For this experiment, I cured droplets of PVDF-trFE in a pre-heated oven set to 130 °C immediately after deposition. These droplets were then cured for different durations ranging from 15-60 minutes. Figure 3.5 shows that the

uniformity does not significantly vary from each duration and that the curing duration could then be reduced to 15 minutes for future samples.

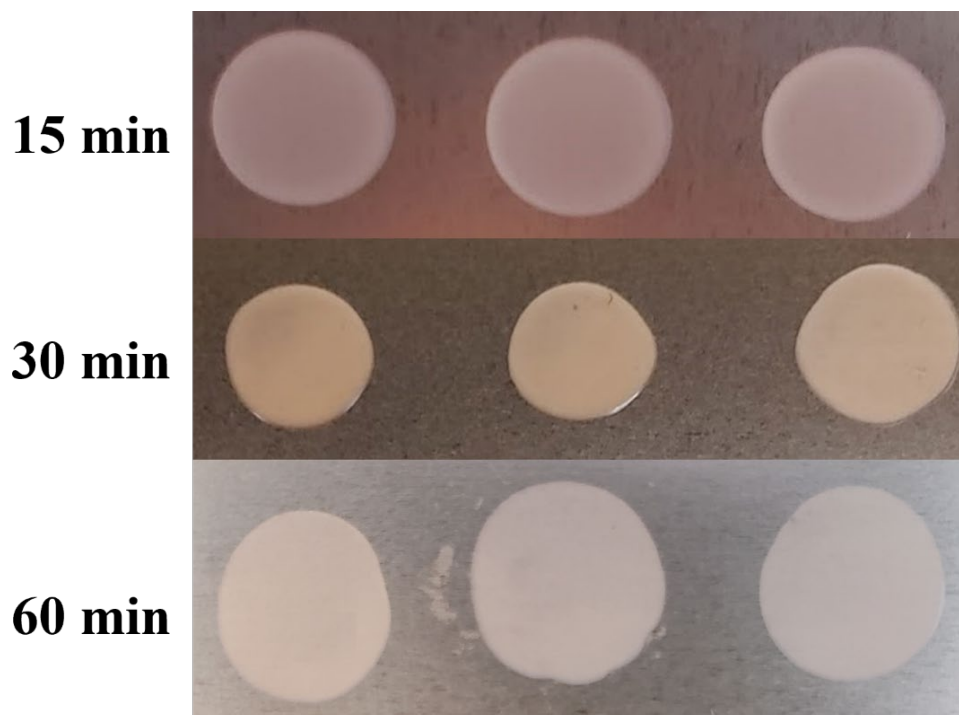


Figure 3.5 Effect of Curing Duration Ranging from 15-60 Minutes

Lastly, I investigated the effect of curing temperature on film uniformity. For this experiment, I utilized the nScribe microdispenser to print 10 mm diameter circles of PVDF-trFE ink atop copper-sputtered silicone wafers. This substrate was utilized in place of copper-coated Kapton so that stylus profilometer (Bruker DektakXT) measurements could be obtained on a flat surface. First, the printed sample was cured in the pre-heated oven set to 130 °C for 15 minutes immediately after deposition. An optical image and profilometer map measurement of the resulting sample was then obtained, shown in pictures (a) and (b) of Figure 3.6. The surface uniformity of this printed sample varied significantly across various points along the film determining this curing temperature unsuitable for sensor development. To determine a more suitable curing temperature, the

boiling points of the ink solvents were then taken into consideration. The boiling point of MEK and DMSO are ~ 80 °C and ~ 189 °C, respectively. First, I wanted to increase the curing temperature to create more rapid boiling of the chemicals in hopes of developing a more uniform thin film. To increase the temperature and still avoid the critical heat flux point of DMSO, I then cured another printed sample at 170 °C. Pictures (c) and (d) from Figure 3.6 show the resulting sample. This temperature yielded a much more uniform film. However, from one side of the printed film to the other, the thickness gradually varied from 30 to 50 μm thick. This inconsistency across the printed film is still unsuitable for sensor development so I then tested a temperature closer to the boiling point of MEK and much lower than DMSO. Avoiding the critical heat flux point of MEK, I cured a printed sample at 90 °C. Pictures (e) and (f) from Figure 3.6 show the much more uniform resulting sample. I then printed and cured more samples utilizing this curing temperature and was able to consistently obtain uniform films approximately 50 μm thick therefore accomplishing the goal of this objective.

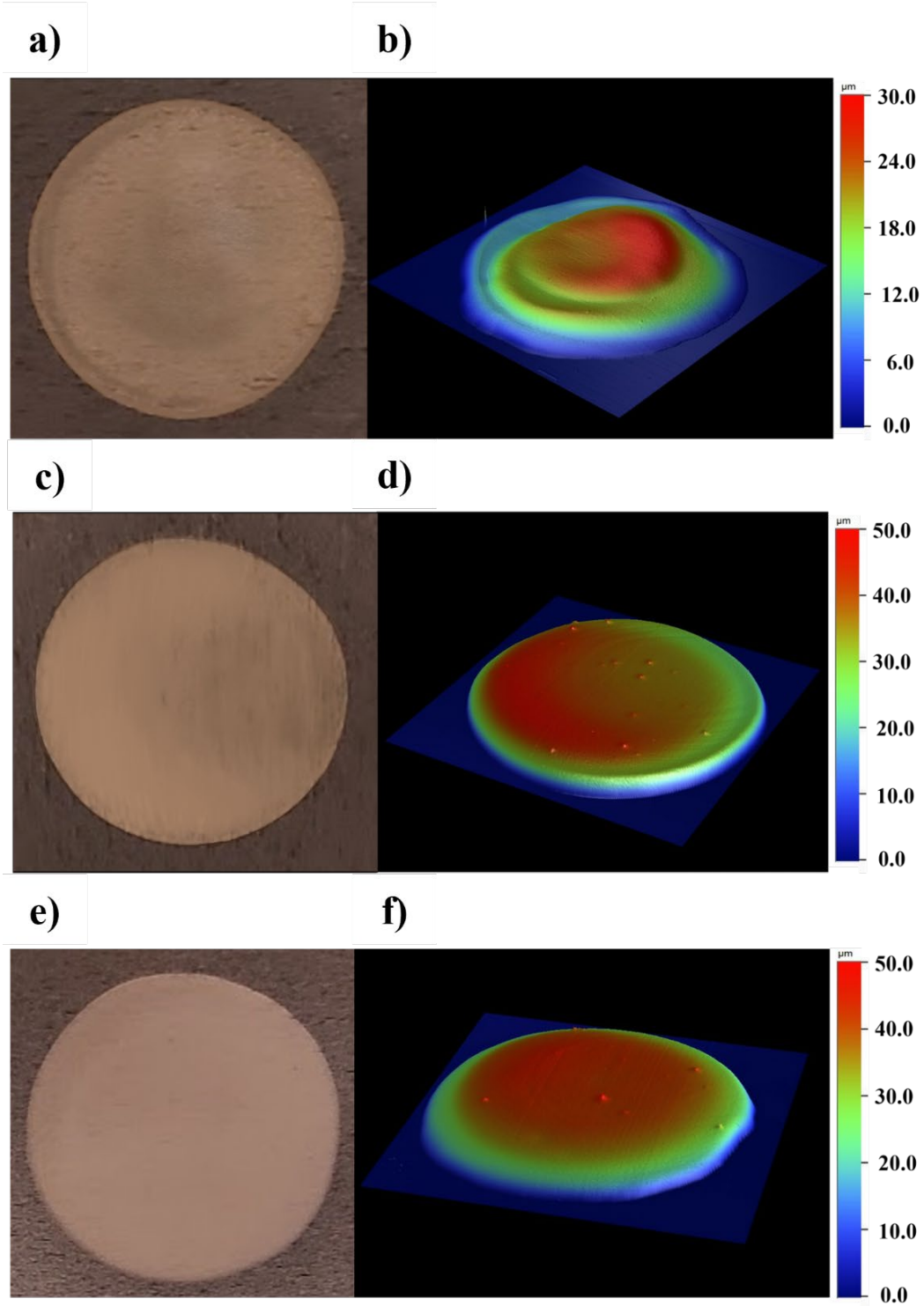


Figure 3.6 Investigation of Curing Temperature with Optical Images (a, c, e) and Profilometer Measurements (b, d, f). Temperatures Investigated Include 130 °C, 170 °C and 90 °C for (a-b), (c-d) and (e-f) Respectively

Future Work

To gain a better understanding of the PVDF-trFE ink developed in this study, contact angle measurements can be performed. As depicted in Figure 3.7, the contact angle measurement is a qualitative way to evaluate how a sample of ink interacts with the substrate surface. By measuring the contact angle of droplets of ink on different substrate materials, optimal substrates may be determined for future piezoelectric sensor development.

- Copper Coated Kapton Substrate
- PVDF-trFE Printed Layer



Figure 3.7 Illustration of Various Contact Angle Measurements

Another investigation that can be conducted toward this objective includes thermogravimetric analysis (TGA) and differential scanning calorimetry (DSC). TGA is a method used to measure the mass of a sample over time as temperature changes. DSC is a method that measures the amount of heat required to increase the temperature of a sample. By completing these two experiments on samples of PVDF-trFE ink, the optimal air-drying, curing temperature and duration can be scientifically measured. This would therefore confirm the optimal air-drying and curing conditions developed in this objective or determine more ideal conditions.

Objective 2: Investigate Effect of Printing Parameters

Summary

To develop uniform printed piezoelectric films utilizing the nScript microdispenser, an investigation of the effects of each printing parameter was conducted. The major printing parameters effecting line width and height include printing pressure, speed, and valve delta. The successful completion of this objective was achieved by determining optimized printing parameters to consistently produce uniform PVDF-trFE films.

Completed Work

To print the 10 wt.% PVDF-trFE ink via the nScript microdispenser system, initial parameters, described in Table 3.2, were utilized. These five parameters determine the overall line quality that can be printed by the nScript microdispenser. The nozzle diameter relates to the diameter of the print tip attached to the print head, which can be changed. This parameter determines the range of line width that can be obtained. For the purpose of printing larger designs for PVDF-trFE film development, the 300 μm diameter nozzle was utilized. The printing speed relates to how fast the print head moves while the design is printed and has a significant effect on line width. The printing pressure relates to how much compressed air is utilized to push ink, from a syringe, through the print head. The pump valve-closed position and valve delta relate to the position of the valve plunger, varying the amount of ink extruded through the print tip. Ethylene propylene diene monomer rubber O-rings were used within the printer assembly, ensuring compatibility with the chemicals in the ink. Directly before printing, substrates underwent acetone bath surface treatment to cleanse the print areas of any oils or debris.

Table 3.2 Initial Printer Settings for 10 wt.% PVDF-trFE Inks

Nozzle Diameter (μm)	Speed (mm/s)	Pressure (kPa)	Valve Closed Position (mm)	Valve Delta (mm)
300	7	68.95	1.82	0.03

Utilizing the printing parameters described in Table 3.2, 10 mm long squares were printed and cured utilizing the optimized curing conditions determined in objective 1. Figure 3.8 displays the resulting squares in which film uniformity is very inconsistent. These results then prompted the need for a thorough investigation and optimization of each printing parameter.

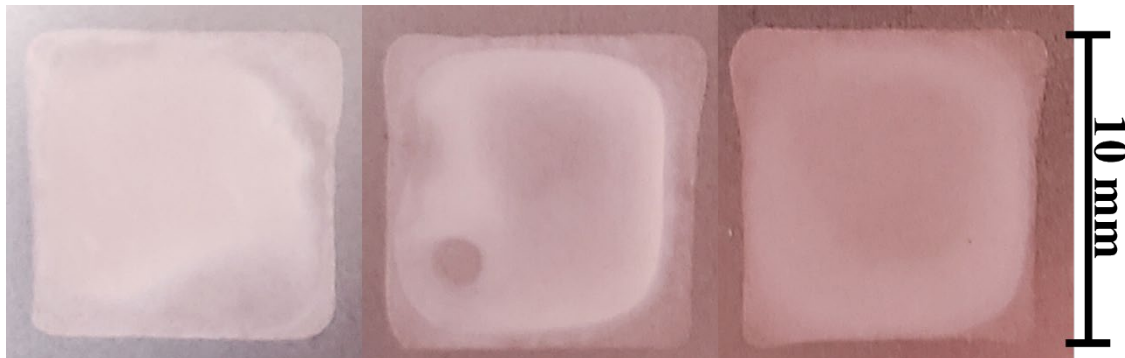


Figure 3.8 nScript Printed 10 wt.% PVDF-trFE Films Utilizing Initial Printing Parameters from Table 3.2

To conduct the printer setting investigation, 10 mm long lines were printed with corresponding experimental parameters on copper-sputtered silicone wafers and then immediately cured for 15 min in a pre-heated 90 °C oven, based on optimized parameters developed in objective 1. The stylus profilometer was then utilized to measure the height and width at ten points along the printed lines. These ten measurements were then averaged. Figure 3.9 displays these results for the corresponding experiment with error bars showing the range of line height and width around those average points.

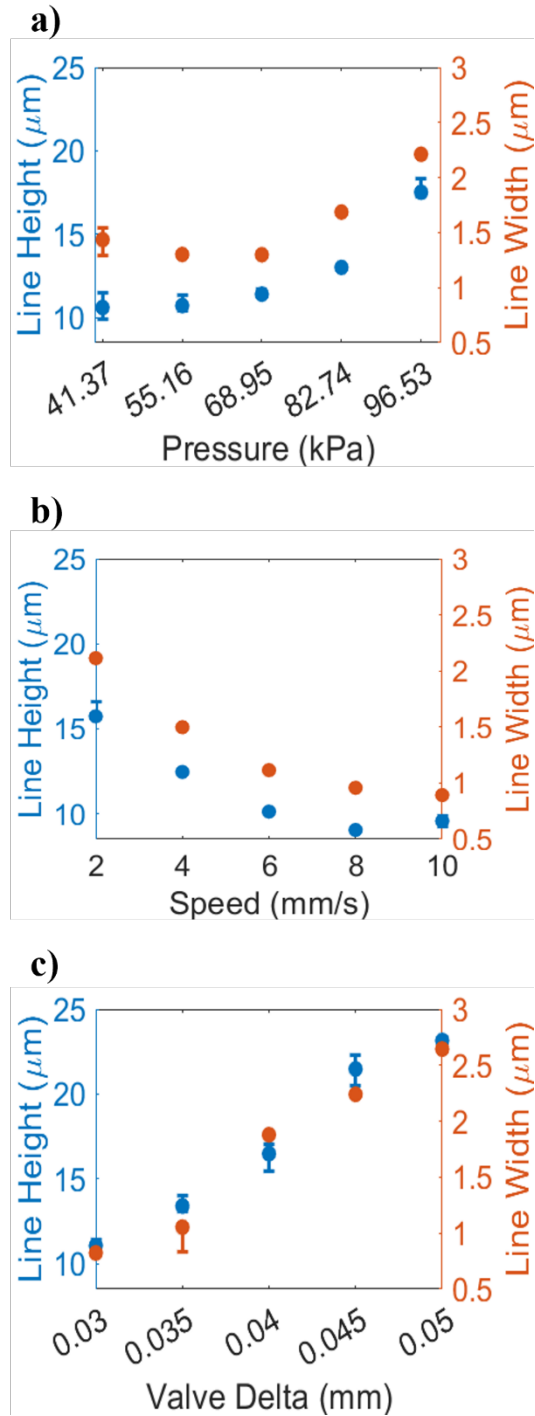


Figure 3.9 Printer Setting Investigation: Average Line Height and Width for Varying (a) Pressure, (b) Speed and (c) Valve Delta

First, the impact of printing pressure, ranging from 41.37 to 96.53 kPa in 13.79 kPa steps, was analyzed. This range was chosen to represent typical low to high printing

pressures with 68.95 kPa being a commonly utilized standard pressure. In this experiment, a printing speed of 6 mm/s and valve delta of 0.04 mm were used. As seen in Figure 3.9, this experiment showed that pressure primarily effected the height of printed lines but also had the most minimal effect on both line height and width.

Second, the impact of printing speed, ranging from 2 to 10 mm/s in 2 mm/s steps was analyzed. This range was chosen to represent typical low to high printing speeds. In this experiment, a printing pressure of 68.95 kPa and valve delta of 0.04 mm was used. As seen in Figure 3.9, this experiment showed that speed had a large impact on both the height and width of printed lines.

Third, the impact of printing valve delta, ranging from 0.03 to 0.05 mm in 0.005 mm steps was analyzed. This range was chosen to represent typical low to high printing valve deltas. In this experiment, a printing speed of 6 mm/s and pressure of 68.95 kPa were used. As seen in Figure 3.9, this experiment showed that valve delta had the most significant and linear impact on both the height and width of printed lines.

From conducting this investigation, optimized printing parameters were determined, as shown in Table 3.3. By utilizing a lower printing speed and larger valve delta, thicker and more consistent printed PVDF-trFE films were obtained.

Table 3.3 Optimized Printer Settings for 10 wt.% PVDF-trFE Inks

Nozzle Diameter (μm)	Speed (mm/s)	Pressure (kPa)	Valve Closed Position (mm)	Valve Delta (mm)
300	6	68.95	1.82	0.04

A stylus profilometer map scan was then obtained in order to confirm surface uniformity of printed films with these parameters. For this measurement, 10 wt.% PVDF-

trFE inks were printed in 10 mm diameter circles on copper-sputtered silicone wafers utilizing the printing parameters listed in Table 3.3. To produce Figure 3.10, a stylus radius of 12.5 μm , 5 mg force and map resolution of 6 $\mu\text{m}/\text{trace}$ was utilized. Some minor surface non-uniformities can be seen and are suspected to be caused by dust particles trapped within the annealed PVDF-trFE film.

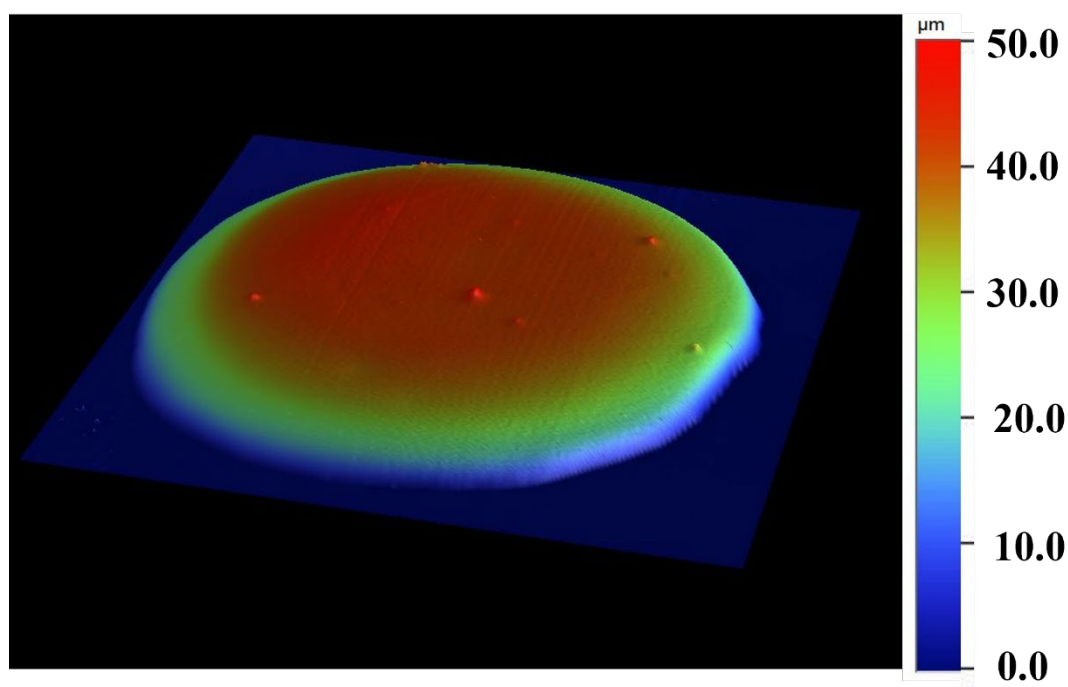




Figure 3.10 Map Scan of a 10 mm Diameter PVDF-trFE Print

From completing these three experiments and performing map scan measurements on PVDF-trFE printed films, utilizing the printing parameters described in Table 3.3, uniform films were produced consistently. The average thickness of these printed samples measured $\sim 40\text{-}50$ μm thick, fulfilling this objective.

Future Work

To gain a better understanding of how the nScript microdispenser parameters can be further optimized, a study of design line spacing can be conducted. As shown in

Figure 3.11, designs printed via the nScript can utilize different line spacings throughout a print. Designs printed throughout this study utilized a line spacing of 0.1 mm. By utilizing different line spacings, designs have the possibility of being produced faster and using less ink. By utilizing less ink, the thickness of cured samples may also change so the printing parameters optimized in this objective could also require optimization for different line spacings. Completing this investigation would yield a better understanding of how varying each nScript parameter can yield a thin film with the same quality and thickness.

-  Copper Coated Kapton Substrate
-  PVDF-trFE Printed Layer

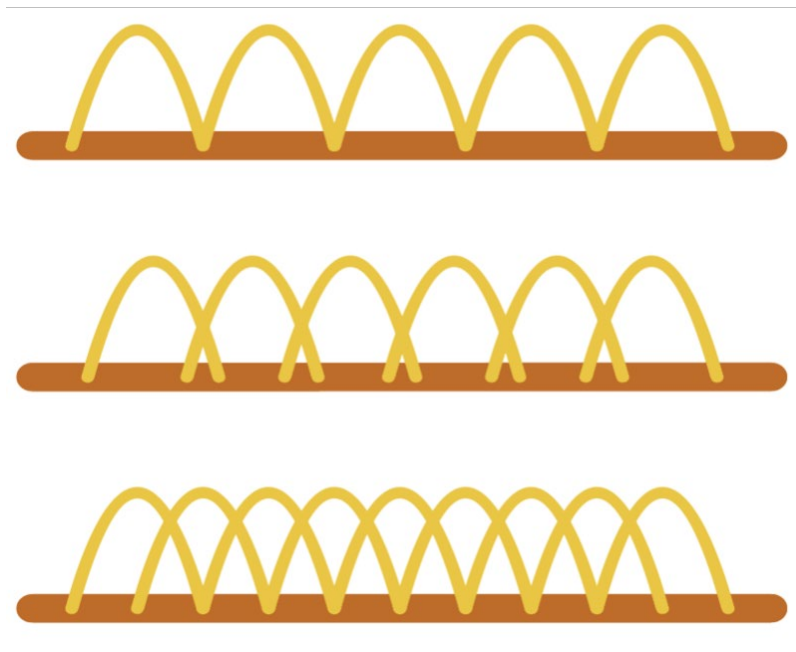


Figure 3.11 Illustration of Various Line Spacing for a Printed Design

Objective 3: Optimize Post-Processing Procedures

Summary

To produce piezoelectric force sensors that match the functionality of commercially available products, post-processing procedures needed to be optimized to facilitate beta phase transformation of uniform cured sensors. The most important post-processing procedure is electrical poling which effects piezoelectric sensitivity and has not been studied in depth by other researchers. An investigation of PVDF-trFE compatible silver inks was also conducted to choose an optimal printable electrode material. The successful completion of this objective was achieved by determining optimized parameters for electrical poling procedures that may be used to consistently achieve d_{33} measurements of 25-30 pC/N for all printed samples.

Completed Work

Once uniform PVDF-trFE thin films were developed consistently, I then printed a silver electrode on top of the cured PVDF-trFE thin film to complete the sandwich structure presented in Figure 2.1. Limited by the low softening temperature of PVDF-trFE [37], the silver ink needs to be sintered below 150 °C. Silver inks that satisfy the sintering temperature limit include Dupont 5029 screen printable silver ink, Applied Ink Solutions WB-1078 water-based silver ink, and NovaCentrix Metalon HPS-FG77 screen printable silver ink as seen printed in Figure 3.12. Other considerations in silver ink selection included ease of printing and chemical compatibility. The Dupont 5029 ink resulted in great uniformity. However, it eroded away the printed PVDF-trFE films causing the printed electrode and the copper-coated Kapton substrate to short. Conversely, the Applied Ink Solutions ink was chemically compatible with the PVDF-

trFE layer, as it is water based. However, this ink was found to be very difficult to print. While printing with this ink, the nozzle would quickly and constantly clog due to the quick drying time of the ink. This resulted in scattered globules of ink. The NovaCentrix ink was easy to print and resulted in uniform electrode prints while also being chemically compatible with the PVDF-trFE layer. Therefore, it was selected amongst the three inks as the top electrode material.

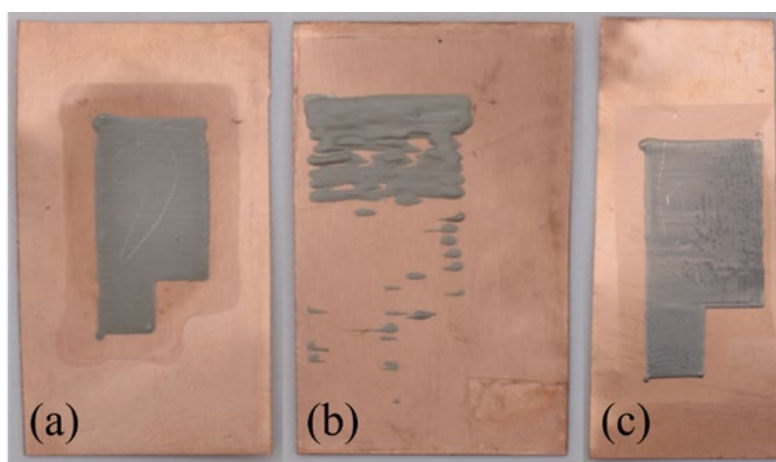


Figure 3.12 Comparison of nScript Printed Electrodes for Three Different Silver Inks: (a) Dupont 5029 Ink, (b) Applied Ink Solutions Water-Based Ink, and (c) NovaCentrix Metalon Ink

In order to consistently print sensor electrodes in thin uniform flexible layers, Table 3.4 displays the optimized silver electrode printing parameters for the NovaCentrix silver ink determined by trial and error. The specifications for this silver ink require curing at 140 °C for 5 minutes.

Table 3.4 Optimized Printer Settings for Silver Electrode

Nozzle Diameter (μm)	Speed (mm/s)	Pressure (kPa)	Valve Closed Position (mm)	Valve Delta (mm)
100	9	68.95	1.82	0.035

Applying an electrical field (100 MV/m) while heating up the PVDF-trFE film near its Curie temperature (~ 80 °C), also known as electrical poling, is a necessary post-processing procedure to convert the as-cured alpha phase PVDF-trFE to the polarized beta phase. To successfully pole the force sensors developed in this study, a commercial electrical poling setup (PolyK Technologies) was submerged in a silicone oil bath atop a hot plate (Thermo Scientific Type 1900), as shown in Figure 3.13. This setup allowed for an even temperature distribution and successful poling of samples. The PVDF-trFE sensors were then sandwiched in between an acorn nut shaped pin, connected to the high voltage amplifier, and a grounded plate. Note that the substrate material utilized in this study is a single sided copper-coated Kapton, so in order to ground this substrate an aluminum shim was used to connect the substrate to the grounded plate.

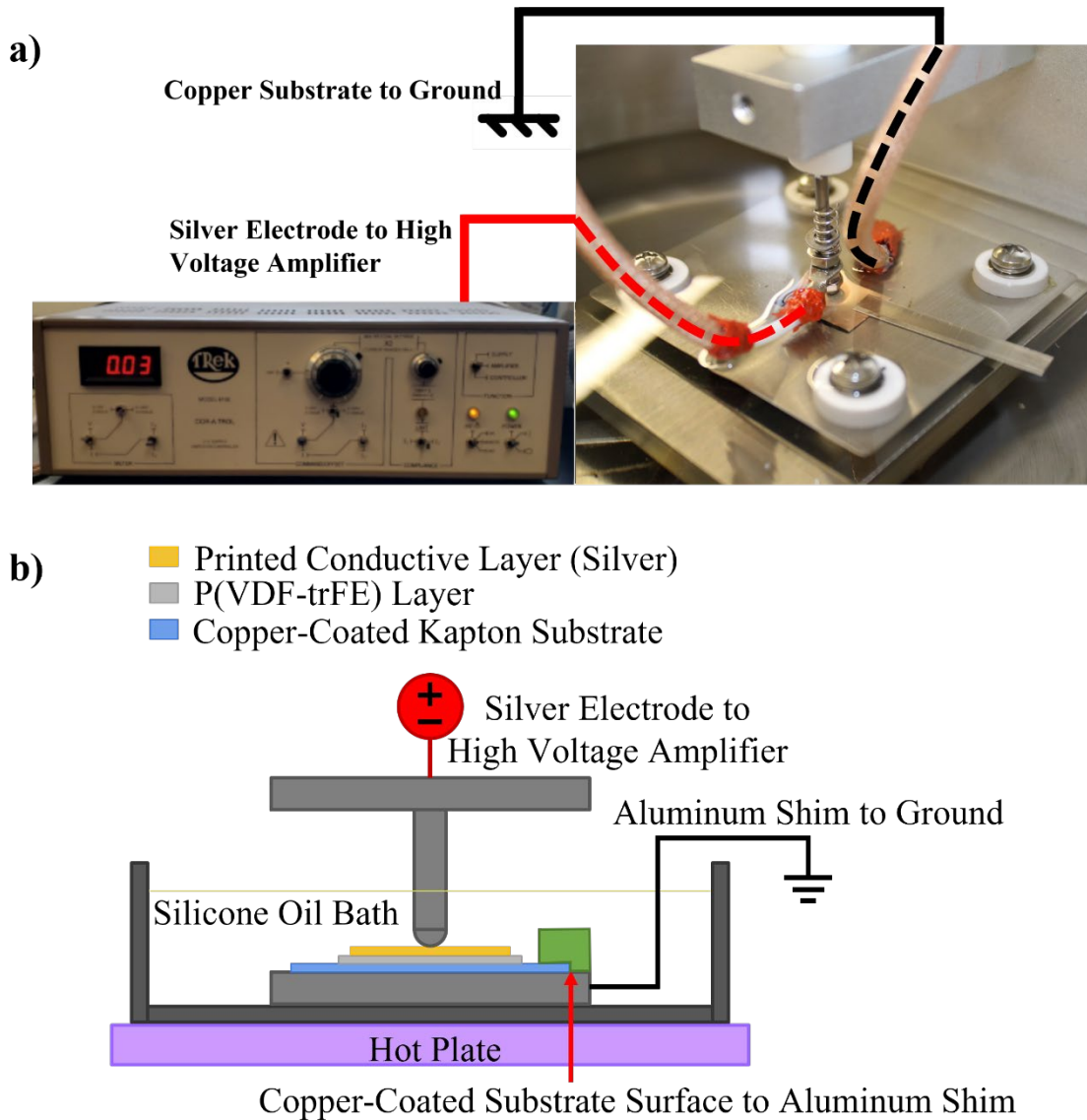


Figure 3.13 Electrical Poling in Silicone Oil Bath: (a) Assembly and (b) Schematic

Based on the overall thickness of the annealed PVDF-trFE layer, $\sim 40\text{-}50\ \mu\text{m}$, the required driving voltage was estimated to be $\sim 5\ \text{kV}$ to generate a strong electric field. To determine the best combination of poling parameters, a study varying the poling voltage, temperature and duration was performed. In each experiment, five samples were tested to determine an average d_{33} value. A commercial d_{33} meter in conjunction with a force transducer and d_{33} shaker (PolyK Technologies) was utilized to accurately measure the d_{33} value of poled sensors, as shown in Figure 3.14.

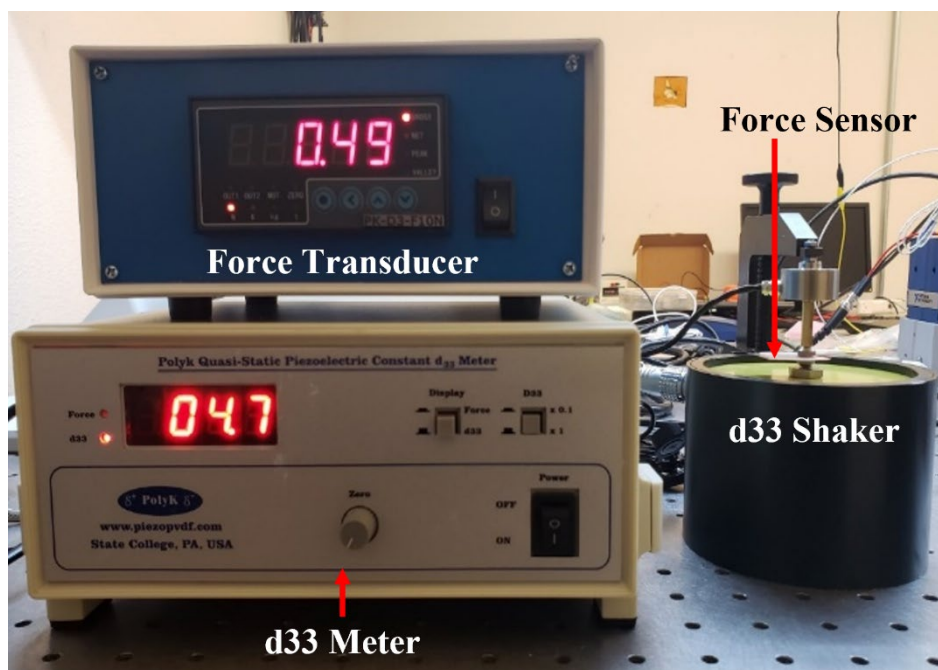


Figure 3.14 Commercial d33 Measuring Setup

The parameter known to have the largest effect on piezoelectric sensitivity is poling voltage. Poling voltage directly correlates to the electric field generation which converts the as-cured alpha phase PVDF-trFE to the polarized beta phase. To test a range of voltages, this study tested poling at 4 to 8 kV in 1 kV steps. Temperature is another important parameter that has a large effect on beta phase transformation in PVDF-trFE films. Limited by the Curie temperature of PVDF-trFE, temperatures tested in this experiment ranged from 20 to 60 °C in 20 °C steps. The last major parameter, duration, has a less significant effect on piezoelectric sensitivity. Based on common poling durations utilized in other studies [38-40], sensors were poled for 5-, 10- and 30-min durations. The results of this experiment are shown in Figure 3.15.

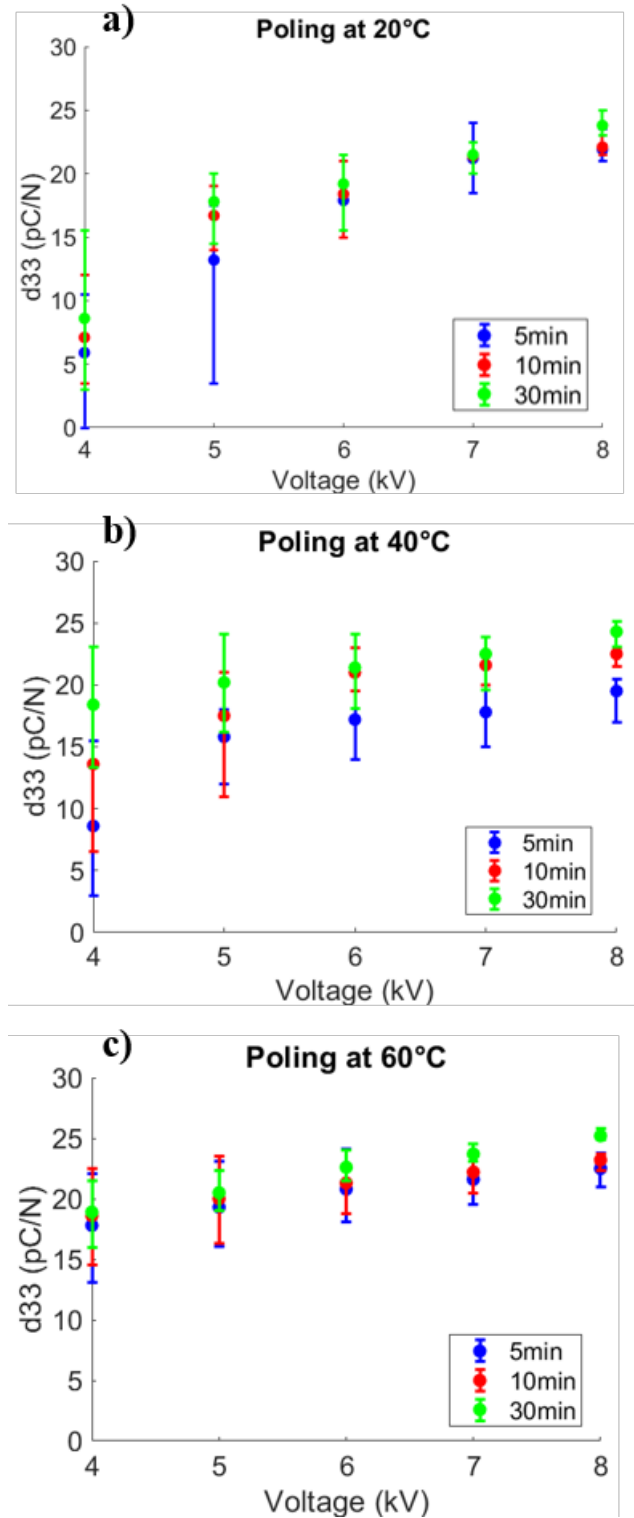


Figure 3.15 Results of Electrical Poling Study Analyzing Driving Voltage and Poling Duration Conducted at (a) 20 °C, (b) 40 °C, and (c) 60 °C

From this experiment, driving voltage was confirmed to have the most significant effect on d_{33} value while poling duration was confirmed to have a minimal effect. Poling temperature was determined to have a significant effect on d_{33} consistency as the range around the average d_{33} values decreased as temperature increased. Results from this experiment confirm that poling sensors at 60 °C for 30 min under a driving voltage of 8 kV yielded the highest d_{33} values, of approximately 26 pC/N, consistently, therefore accomplishing this objective.

Future Work

To limit film breakdown of sensors during the poling process, non-contact corona poling was briefly investigated. Figure 3.16 displays the corona poling setup in which a tungsten needle (McCrone Group #2 SHARP) is connected to a high voltage amplifier (Trek Model 610E) with its tip situated ~2 cm above the sample. It was discovered that samples with printed silver electrodes would cause streamer discharges from the needle tip to the electrodes and quickly break down the sandwiched PVDF-trFE films. For this reason, corona poling was determined to be unsuitable for electrical poling of sensors in this study. However, this electrical poling method is also more tolerable of PVDF-trFE film non-uniformities and can be utilized for electrical poling of sensors without printed electrodes. Therefore, an in-depth study of electrical poling parameters including driving voltage, poling temperature, poling duration, and needle tip distance could be beneficial for future researchers.

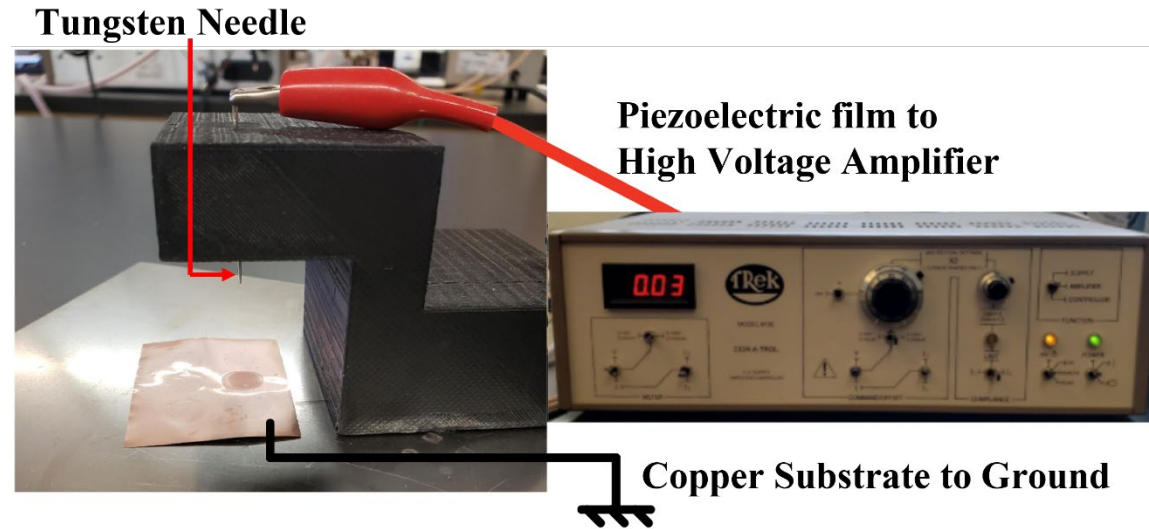


Figure 3.16 Non-Contact Corona Poling Assembly

Other work that can be conducted towards this objective includes performing Fourier-transform infrared spectroscopy (FTIR). FTIR is a technique used to measure infrared spectrum absorption/emission. By performing FTIR analysis on the electrically poled PVDF-trFE films, the exact percentage of beta phase transformation can be determined and confirm the d_{33} values measured in this study.

Objective 4: Prototype and Characterize PVDF-trFE Force Sensors

Summary

To develop dynamic PVDF-trFE force sensors that match the functionality of commercially available products, as well as unprecedented tactile sensor arrays, functional prototypes needed to be produced and characterized. Towards this objective, smaller tasks were developed to analyze each factor. First, task 4.1 focused on designing and prototyping tactile sensor arrays based off previously acquired knowledge of PVDF-trFE sensor formulation. Task 4.2 aimed to measure the functionality of these prototyped tactile sensor arrays. Lastly, task 4.3 aimed to measure force sensor sensitivity to show product functionality. The successful completion of this objective was achieved by

developing a physical tactile sensor array. Along with the physical sensor, the optimized electrode printing procedures and sensor characterization setup were developed.

Completed Work

With the knowledge acquired throughout this study, unprecedented functional tactile sensor array prototypes were produced and characterized. Figure 3.17 displays the tactile sensor array configuration. In this design, a 1D array of printed PVDF-trFE sensors forms a ‘piano’. These sensors were produced utilizing the same printing, curing and poling parameters developed in the previous objectives and not only measure force magnitude but also location of the applied force within the system of sensors.

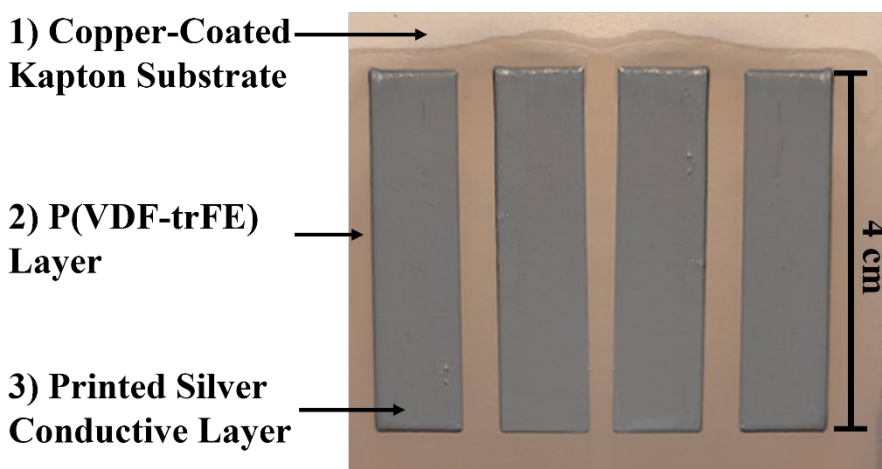


Figure 3.17 Dimensions of PVDF-trFE 1D 'Piano' Sensor Array

To measure the force location sensing of the 1D ‘piano’ array, a custom characterization setup was developed, shown in Figure 3.18. In this setup, the PVDF-trFE sensor array is connected to an Arduino and speaker through a breadboard. Specific music notes are played as force is applied to the corresponding sensors in the array. This setup can also be modified to activate LED lights as force is applied to various sensors in the array.

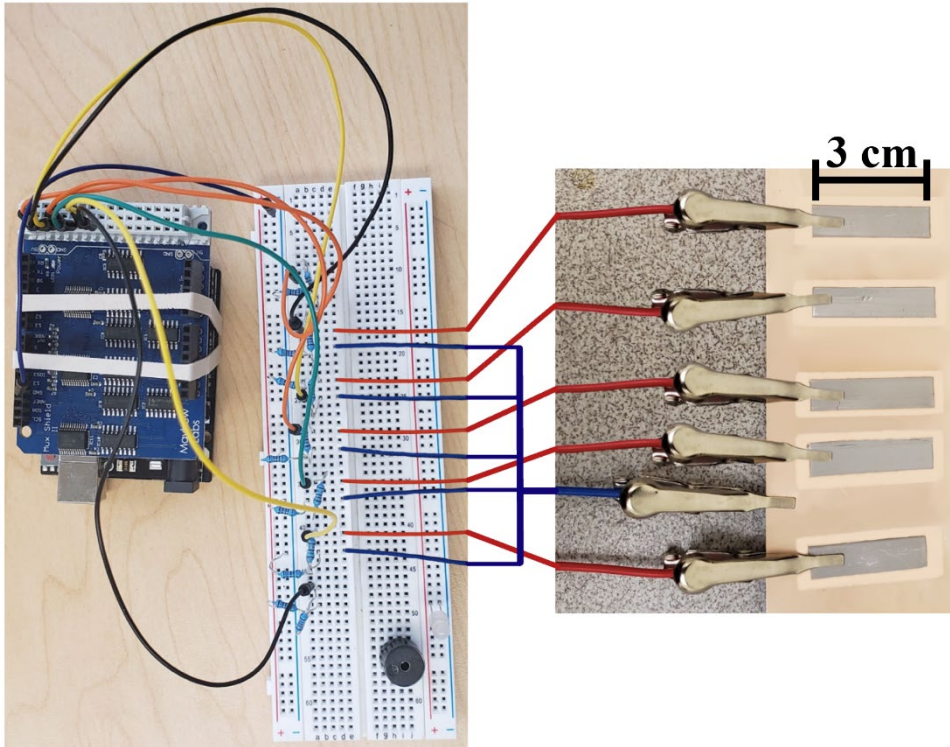


Figure 3.18 Custom Characterization Setup of the 1D 'Piano' Sensor Array

Sensitivity of the printed sensors was tested utilizing a custom load frame setup, as shown in Figure 3.19, where PVDF-trFE sensors were sandwiched between a piezo stack actuator (ThorLab) with an acorn nut and a piezo force sensor (PCB, model no. 208C02). The piezo actuator was driven by a high voltage power amplifier (PI, model no. E-501.00) and a DC voltage of 500 V was applied to prevent the actuator from operating in negative voltages.

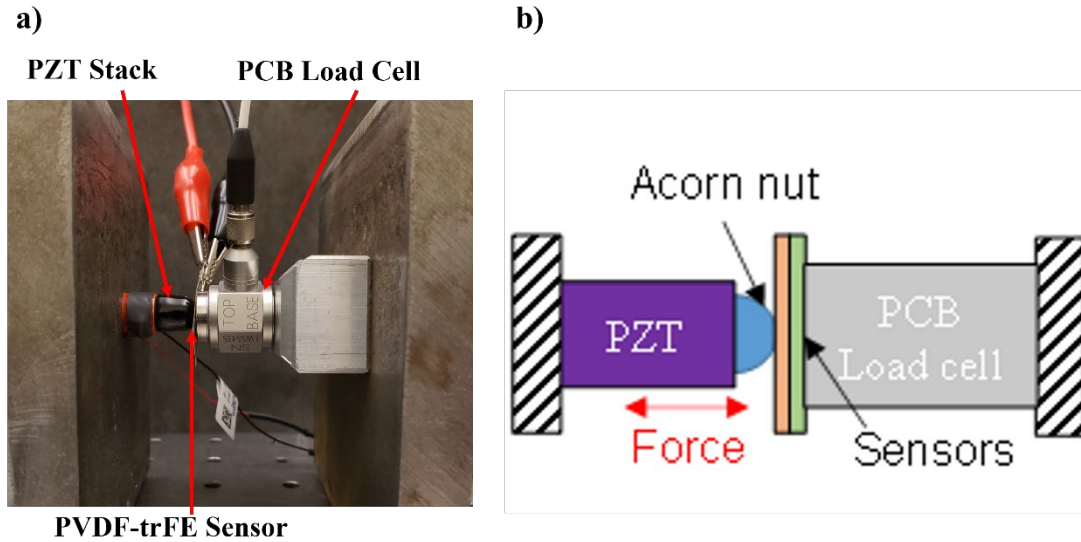


Figure 3.19 Customized Load Frame Setup (a) and Schematic (b) Showing Printed Sensors Sandwiched Between a PZT Actuator and Piezo Force Sensor

An AC voltage with a magnitude of 100 V was added on top of the DC voltage to generate the dynamic force excitation. The frequency of the AC voltage was controlled by a data acquisition system (Data Physics, model no. DP240). The resulting electrical voltage across the PVDF-trFE sensor $V(t)$ and the reference force measured by the piezo load cell $F(t)$ were recorded by the same data acquisition system. The sensitivity was calculated as

$$S = V_0/F_0 \quad (1)$$

where V_0 and F_0 are the magnitudes of the fundamental component of $V(t)$ and $F(t)$, respectively. Figure 3.20 shows the sensitivity of the printed sensor measured at various excitation frequencies compared to the sensitivity of a commercial sensor (TE Connectivity). For frequencies beyond 2 kHz, the sensitivity stabilized at around 1-1.2 V/N. Overall, the printed sensor developed in this study was determined to be significantly more sensitive than its commercial counterpart.

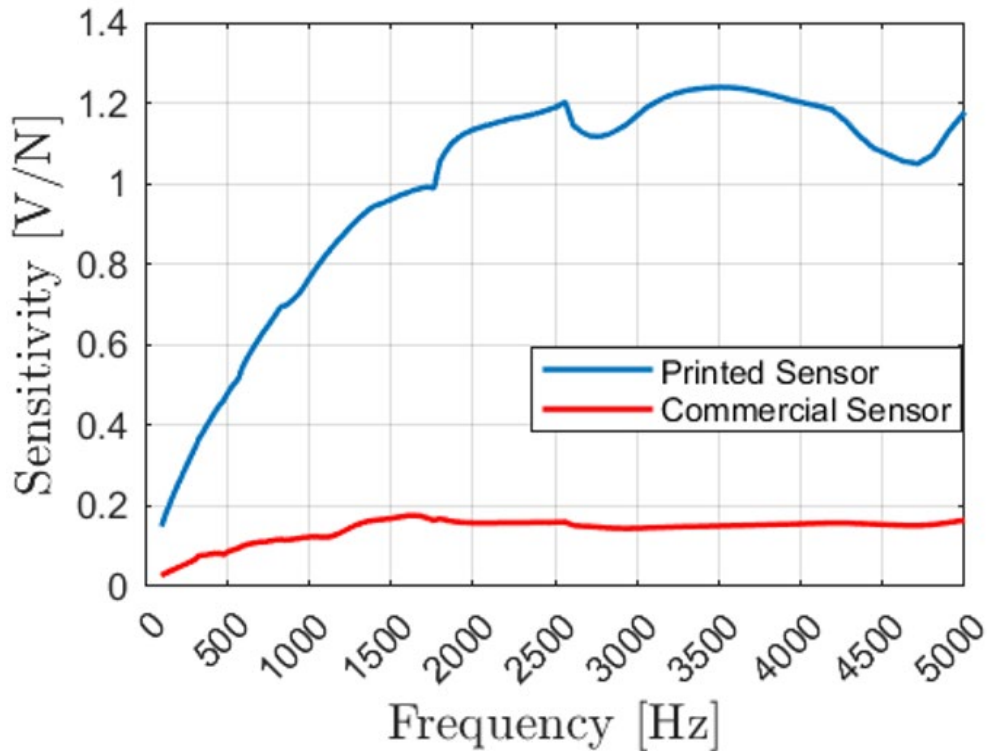


Figure 3.20 Sensitivity (V/N) vs. Frequency (Hz) of nScript Printed, Electrically Poled Sensors Compared to Commercial PVDF-trFE Sensor

The voltage response of the printed PVDF-trFE sensor was also measured in Figure 3.21 at 2 and 5 kHz. From these plots we see that the voltage response nearly matched the sinusoidal force applied to the sensor at both frequencies showing the efficiency of the sensors developed in this study. By developing both force sensors as well as tactile sensor arrays with increased sensitivity to their commercial counterparts, this objective was accomplished.

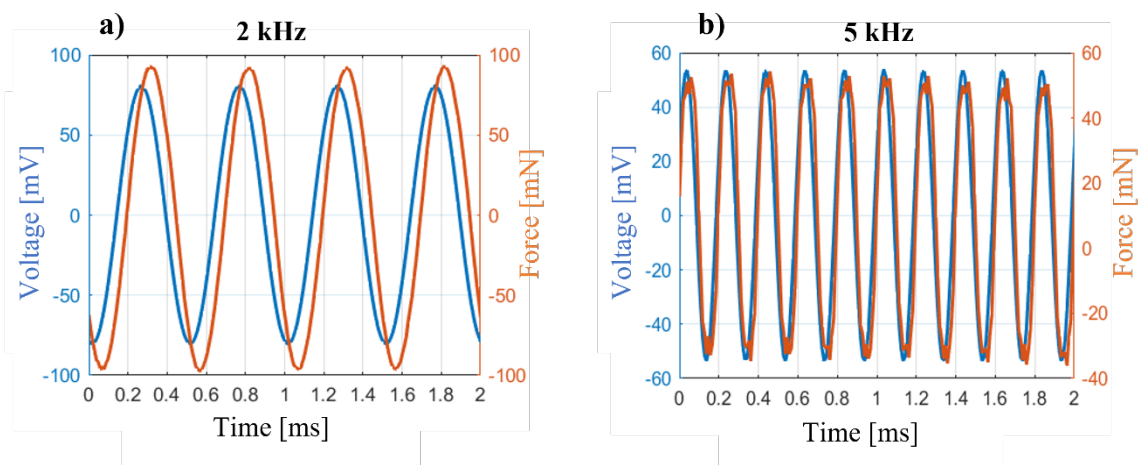


Figure 3.21 Electrical Response of Printed PVDF-trFE Sensor Over 2 ms at (a) 2 kHz and (b) 5 kHz

Future Work

Additional work that can be conducted toward this objective includes the further study of tactile sensor arrays. In this study a 1D array was developed, however more complex sensor systems in 2D can be developed. Figure 3.22 displays a prototype of a 2D 2 × 2 sensor array that has the capability of measuring where within the sensor system a force is applied. This kind of sensor array can be further developed into 3 × 3 arrays or more.

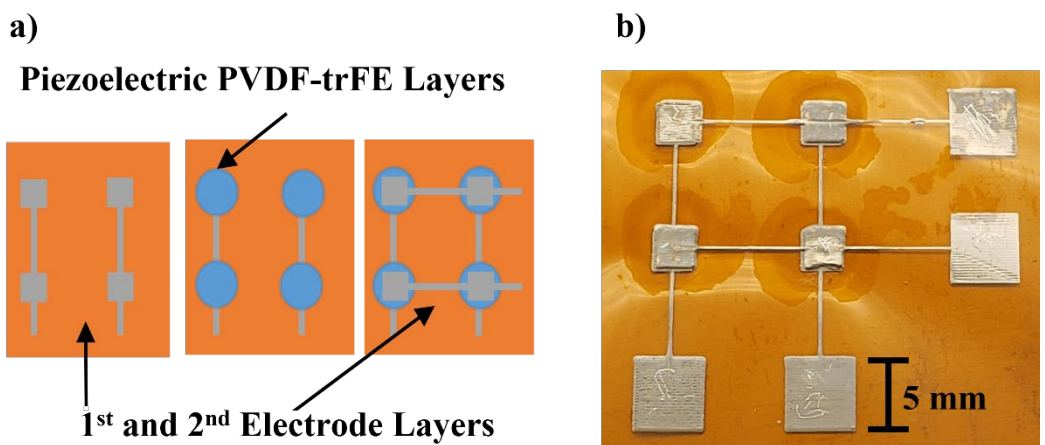


Figure 3.22 2D Sensor Array (a) Schematic and (b) Prototype

Conclusion

This investigation aimed to develop unprecedented, all-printed PVDF-trFE piezoelectric force sensors by utilizing an nScript microdispenser. This piezoelectric material was chosen for its good piezoelectric sensitivity, ductility, high mechanical strength, biocompatibility and chemical resistance. This printing method was chosen for its range of viscosity, complex design capabilities, fast optimization and low waste production.

For this study, a custom 10 wt.% PVDF-trFE ink was developed using PVDF-trFE powders dissolved in a cosolvent system of MEK and DMSO. Uniform films were developed by analyzing the effects of air-drying, curing duration and curing temperature. To consistently yield uniform PVDF-trFE films, the optimal ink preparation included immediate curing for 15 min and a pre-heated 90 °C oven after deposition onto acetone cleaned copper-coated Kapton substrates.

An investigation of nScript microdispenser printing settings was then conducted varying printing pressure, speed and valve delta. From this investigation, valve delta was determined to have the most significant effect on line height and width. To consistently produce PVDF-trFE films ~40-50 μm thick, printer settings, listed in Table 3.3, were optimized based off this investigation.

Post-processing procedures, focusing on electrical poling, were then investigated, and optimized to facilitate beta phase transformation and increase piezoelectric sensitivity. Electrical poling driving voltage, temperature and duration were analyzed to determine the combination that yielded the highest d_{33} value. Sensors consistently measured a d_{33} value of 26 pC/N when poled at 60 °C at 8 kV for 30 min.

Prototyped force sensors and unprecedented tactile sensor arrays were developed with their corresponding sensitivity measured utilizing custom characterization setups. The sensitivity was then compared to commercial products and determined to have significantly higher sensitivity stabilizing around 1.1 V/N.

REFERENCES

- [1] Zeiser, R., Fellner, T., & Wilde, J. 2014. *Capacitive strain gauges on flexible polymer substrates for wireless, intelligent systems*. Journal of Sensors and Sensor Systems, 3(1), 77-86.
- [2] Hay, G. I., Evans, P. S., Harrison, D. J., Southee, D., Simpson, G., & Harrey, P. M. 2005. *Characterization of lithographically printed resistive strain gauges*. IEEE Sensors Journal, 5(5), 864-871.
- [3] Fiorillo, A. S., Critello, C. D., & Pullano, S. A. 2018. *Theory, technology and applications of piezoresistive sensors: A review*. Sensors and Actuators A: Physical, 281, 156-175.
- [4] Jia, N., He, Q., Sun, J., Xia, G., & Song, R. 2017. *Crystallization behavior and electroactive properties of PVDF, P (VDF-TrFE) and their blend films*. Polym. Test. 57 302-6.
- [5] Dahiya, R. S., Valle, M., Metta, G., Lorenzelli, L., & Pedrotti, S. 2008. *Deposition, processing and characterization of P (VDF-TrFE) thin films for sensing applications*. IEEE Sens.: Conf. Ser. 2008 490-3.
- [6] Cho, Y., & et al. 2015. *Enhanced energy harvesting based on surface morphology engineering of P (VDF-TrFE) film*. Nano Energy 16 524-32.
- [7] McGinn, C. K., Kam, K. A., Laurila, M. M., Lozano Montero, K., Mäntysalo, M., Lupo, D., & Kymissis, I. 2020. *Formulation, printing, and poling method for piezoelectric films based on PVDF-TrFE*. Int. J. Appl. Phys. 128 225304.
- [8] Marandi, M., & Tarbutton, J. 2019. *Additive manufacturing of single-And double-layer piezoelectric PVDF-TrFE copolymer sensors*. Procedia Manuf. 34 666-7.

- [9] Porter, D. A., Hoang, T. V., & Berfield, T. A. 2017. *Effects of in-situ poling and process parameters on fused filament fabrication printed PVDF sheet mechanical and electrical properties*. *Addit. Manuf.* 13 81-92.
- [10] Beringer, L. T., Xu, X., Shih, W., Shih, W. H., Habas, R., & Schauer, C. L. 2015. *An electrospun PVDF-TrFe fiber sensor platform for biological applications*. *Sens. Actuator A Phys.* 222 293-300.
- [11] Abolhasani, M. M., Shirvanimoghaddam, K., Khayyam, H., Moosavi, S. M., Zohdi, N., & Naebe, M. 2018. *Towards predicting the piezoelectricity and physiochemical properties of the electrospun P (VDF-TrFE) nanogenerators using an artificial neural network*. *Polym. Test.* 66 178-88.
- [12] Haque, R. I., Vié, R., Germainy, M., Valbin, L., Benaben, P., & Boddaert, X. 2015. *Inkjet printing of high molecular weight PVDF-TrFE for flexible electronics*. *Flex. Print. Electron.* 1 015001.
- [13] Banquart, A., Callé, S., Levassort, F., Fritsch, L., Ossant, F., Toffessi Siewe, S., Chevalliot, S., Capri, A., & Grégoire, J. M. 2021. *Piezoelectric P (VDF-TrFE) film inkjet printed on silicone for high-frequency ultrasound applications*. *Int. J. Appl. Phys.* 129 195107.
- [14] Closson, A., Richards, H., Xu, Z., Jin, C., Dong, L., & Zhang, J. X. 2021. *Method for Inkjet-printing PEDOT: PSS polymer electrode arrays on piezoelectric PVDF-TrFE fibers*. *IEEE Sens. J.* 21 26277-85.
- [15] *Market Research Future*. 2021. Polyvinylidene Fluoride (PVDF) Market Size, Growth, Trends, Global Overview.
<https://www.marketresearchfuture.com/reports/polyvinylidene-fluoride-market-4472>.
- [16] Li, Y., Feng, W., Meng, L., Tse, K. M., Li, Z., Huang, L., ... & Guo, S. 2021. *Investigation on in-situ sprayed, annealed and corona poled PVDF-TrFE coatings for guided wave-based structural health monitoring: From crystallization to piezoelectricity*. *Materials & Design*, 199, 109415.

- [17] Curry, E. J., Ke, K., Chorsi, M. T., Wrobel, K. S., Miller, A. N., Patel, A., ... & Nguyen, T. D. 2018. *Biodegradable piezoelectric force sensor*. Proceedings of the National Academy of Sciences, 115(5), 909-914.
- [18] Altintas, Y., & Park, S. S. 2004. *Dynamic compensation of spindle-integrated force sensors*. CIRP Annals, 53(1), 305-308.
- [19] Yamada, T., Niizeki, N., & Toyoda, H. 1967. *Piezoelectric and elastic properties of lithium niobate single crystals*. Japanese Journal of Applied Physics, 6(2), 151.
- [20] Lueng, C. M., Chan, H. L., Surya, C., & Choy, C. L. 2000. *Piezoelectric coefficient of aluminum nitride and gallium nitride*. Journal of applied physics, 88(9), 5360-5363.
- [21] Jerphagnon, J., & Kurtz, S. K. 1970. *Optical nonlinear susceptibilities: accurate relative values for quartz, ammonium dihydrogen phosphate, and potassium dihydrogen phosphate*. Physical Review B, 1(4), 1739.
- [22] Lian, L., & Sottos, N. R. 2000. *Effects of thickness on the piezoelectric and dielectric properties of lead zirconate titanate thin films*. Journal of Applied Physics, 87(8), 3941-3949.
- [23] Guo, Q., Cao, G. Z., & Shen, I. Y. 2013. *Measurements of piezoelectric coefficient d_{33} of lead zirconate titanate thin films using a mini force hammer*. Journal of Vibration and Acoustics, 135(1).
- [24] Yako, K., Kakemoto, H., Tsurumi, T., & Wada, S. 2005. *Domain size dependence of d_{33} piezoelectric properties for barium titanate single crystals with engineered domain configurations*. Materials Science and Engineering: B, 120(1-3), 181-185.
- [25] Shen, Z. Y., & Li, J. F. 2010. *Enhancement of piezoelectric constant d_{33} in BaTiO₃ ceramics due to nano-domain structure*. Journal of the Ceramic Society of Japan, 118(1382), 940-943.
- [26] Dong, W., Xiao, L., Hu, W., Zhu, C., Huang, Y., & Yin, Z. 2017. *Wearable human-machine interface based on PVDF piezoelectric sensor*. Trans. Inst. Meas. Control 39 398-403.

- [27] Kim, H., Torres, F., Wu, Y., Villagran, D., Lin, Y., & Tseng, T. L. B. 2017. *Integrated 3D printing and corona poling process of PVDF piezoelectric films for pressure sensor application*. Smart Mater. Struct. 26 085027.
- [28] Zhang, Q., Liu, S., Luo, H., Guo, Z., Hu, X., & Xiang, Y. 2020. *Hybrid capacitive/piezoelectric visualized meteorological sensor based on in-situ polarized pvdf-trfe films on tft arrays*. Sensors and Actuators A: Physical, 315, 112286.
- [29] You, M., Hu, X., & Xiang, Y. 2021. *In-situ polarization enhanced piezoelectric property of polyvinylidene fluoride-trifluoroethylene films*. In IOP Conference Series: Earth and Environmental Science (Vol. 770, No. 1, p. 012071). IOP Publishing.
- [30] Shintaku, H., Tateno, T., Tsuchioka, N., Tanujaya, H., Nakagawa, T., Ito, J., & Kawano, S. 2010. *Culturing neurons on MEMS fabricated P (VDF-TrFE) films for implantable artificial cochlea*. Journal of Biomechanical Science and Engineering, 5(3), 229-235.
- [31] Sharma, T., Je, S. S., Gill, B., & Zhang, J. X. 2012. *Patterning piezoelectric thin film PVDF-TrFE based pressure sensor for catheter application*. Sensors and Actuators A: physical, 177, 87-92.
- [32] Toprak, A., & Tigli, O. 2015. *MEMS scale PVDF-TrFE-based piezoelectric energy harvesters*. Journal of Microelectromechanical Systems, 24(6), 1989-1997.
- [33] Costa, C. M., Cardoso, V. F., Sencadas, V., Rodrigues, L. C., Silva, M. M., & Lanceros-Méndez, S. 2012. *Electroactive poly (vinylidene fluoride-trifluoroethylene)(PVDF-TrFE) microporous membranes for lithium-ion battery applications*. Ferroelectrics, 430(1), 103-107.
- [34] “Piezotech p(VDF-TrFE) 70/30, 75/25, or 80/20 Mol Copolymer Resin.” Piezoelectric & Pyroelectric PVDF & PVDF-TrFE, Resin, Film, Sensor, Transducer, and Test Instrument, PolyK. 2022. <https://piezopvdf.com/piezotech-PVDF-TrFE-resin-10-gram/>.

- [35] Morales, A. R. R., & Zaghloul, M. E. 2018. *Highly sensitive wearable piezoelectric force sensor with quasi-static load testing*. IEEE Sensors Journal, 18(24), 9910-9918.
- [36] Thuau, D., Kallitsis, K., Dos Santos, F. D., & Hadziioannou, G. 2017. *All inkjet-printed piezoelectric electronic devices: energy generators, sensors and actuators*. Journal of Materials Chemistry C, 5(38), 9963-9966.
- [37] Arifin, D. E. S., & Ruan, J. J. 2018. *Study on the curie transition of P (VDF-TrFE) copolymer*. In IOP Conference Series: Materials Science and Engineering (Vol. 299, No. 1, p. 012056). IOP Publishing.
- [38] Hu, X., Ding, Z., Fei, L., & Xiang, Y. 2019. *Wearable piezoelectric nanogenerators based on reduced graphene oxide and in situ polarization-enhanced PVDF-TrFE films*. Journal of materials science, 54(8), 6401-6409.
- [39] Zhu, G., Xu, J., Zeng, Z., Zhang, L., Yan, X., & Li, J. 2006. *Electric field dependence of topography in ferroelectric P (VDF/TrFE) films*. Applied Surface Science, 253(5), 2498-2501.
- [40] Ducrot, P. H., Dufour, I., & Ayela, C. 2016. *Optimization of PVDF-TrFE processing conditions for the fabrication of organic MEMS resonators*. Scientific reports, 6(1), 1-7.

APPENDIX

Results of Poling Experiments

Table A.1 Results of Poling Experiment Conducted at 20 °C and Measured in pC/N

	4 kV	5	6	7	8
5 min	0.00	3.50	15.0	18.5	21.0
	3.50	14.5	17.5	20.5	21.5
	10.5	16.5	19.5	22.5	21.5
	14.5	17.5	21.0	24.0	23.5
	1.00	14.0	16.5	20.5	22.0
10	4.50	16.0	16.5	21.0	22.5
	11.0	14.0	15.0	20.0	21.5
	3.50	17.0	21.0	22.5	23.0
	4.50	17.5	19.5	21.5	21.5
	12.0	19.0	20.0	22.0	22.0
30	6.00	14.5	15.5	21.0	25.0
	13.0	20.0	21.5	22.5	23.0
	15.5	20.0	21.0	22.0	23.0
	3.00	15.0	17.5	20.0	24.0
	5.50	19.5	20.5	22.0	23.0

Table A.2 Results of Poling Experiment Conducted at 40 °C and Measured in pC/N

	4 kV	5	6	7	8
5 min	6.00	15.0	18.0	18.5	20.5
	4.00	12.0	14.0	15.0	17.0
	3.00	16.0	15.0	16.0	19.0
	15.5	18.0	19.5	20.0	20.5
	14.5	18.0	19.5	19.5	20.5
10	14.5	17.0	19.5	20.0	21.5
	2.50	11.0	19.5	22.5	23.0
	18.0	21.0	22.5	22.5	22.0
	14.5	18.5	20.5	21.0	23.0
	18.5	20.0	23.0	22.0	23.0
30	20.0	21.5	22.5	23.5	25.0
	18.5	20.5	21.5	22.5	24.0
	23.0	24.0	24.0	24.5	25.0
	17.0	19.0	21.0	22.5	24.5
	13.5	16.0	18.0	19.5	23.0

Table A.3 Results of Poling Experiment Conducted at 60 °C and Measured in pC/N

	4 kV	5	6	7	8
5 min	22.0	21.0	22.0	22.5	23.0
	17.5	19.5	21.5	22.0	22.5
	17.0	18.5	20.0	20.5	22.0
	15.0	17.5	19.5	21.0	22.0
	17.5	20.0	21.0	22.0	23.0
10	14.5	16.5	19.0	20.5	22.5
	18.0	19.5	20.5	21.0	21.5
	20.5	22.0	23.5	24.0	24.5
	17.5	18.5	19.5	21.5	23.0
	22.5	23.5	24.0	24.0	24.5
30	20.0	20.5	22.5	23.5	25.0
	21.5	22.5	24.0	24.5	26.0
	16.0	19.0	21.5	23.0	25.0
	19.5	21.0	23.0	24.0	25.0
	17.5	19.5	22.0	23.5	25.0